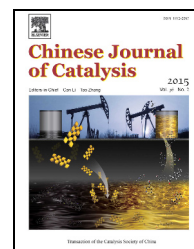


available at www.sciencedirect.comjournal homepage: www.elsevier.com/locate/chnjc

Article

Preparation of magnetic nanocomposites of solid acid catalysts and their applicability in esterification



Huanwang Jing*, Xiaomei Wang, Yong Liu, Anqi Wang

State Key Laboratory of Applied Organic Chemistry, College of Chemistry and Chemical Engineering, Lanzhou University, Lanzhou 730000, Gansu, China

ARTICLE INFO

Article history:

Received 18 June 2014

Accepted 1 September 2014

Published 20 February 2015

Keywords:

Magnetic nanocomposite

Solid acid catalyst

Co-precipitation method

Esterification reaction

ABSTRACT

Solid acid catalysts are superior to traditional liquid acids because they are noncorrosive, environmentally benign, and recyclable. In addition, nano-magnetic solid acid catalysts are preferable as they exhibit large specific surface areas together with good acidity and are also readily separated from the post-reaction mixture. Three component nano-magnetic solid catalysts $\text{TiO}_2\text{-Al}_2\text{O}_3\text{-Fe}_3\text{O}_4$ and $\text{CeO}_2\text{-Al}_2\text{O}_3\text{-Fe}_3\text{O}_4$ and a four component catalyst $\text{ZrO}_2\text{-Al}_2\text{O}_3\text{-CeO}_2\text{-Fe}_3\text{O}_4$ were synthesized by a co-precipitation method and were subsequently characterized by inductively coupled plasma-atomic emission spectroscopy, Brunauer-Emmett-Teller surface area analysis, X-ray diffraction, transmission electron microscopy, and thermal gravimetric analysis. Their catalytic activities were also evaluated in the esterification reaction of acetic acid with *n*-butanol. The results demonstrated that these rare earth-based magnetic nanocomposites exhibited good catalytic activity.

© 2015, Dalian Institute of Chemical Physics, Chinese Academy of Sciences.

Published by Elsevier B.V. All rights reserved.

1. Introduction

Acid catalysts have numerous applications in various industrial organic reactions, and homogenous acids such as H_2SO_4 , HCl , and HF have been widely used in chemical engineering. However, these mineral acids have serious drawbacks in terms of difficulties in post-reaction separation and negative environmental impact, as well as their tendency to contribute to the corrosion of reactors. Over the last few decades, many different solid acid catalysts have been developed as alternatives, including metal oxides, zeolites, metal phosphates, and sulfated metal oxides [1–5], and these are widely used in alkylation [6], esterification [7,8], isomerization [9,10], nitration [11], and other reactions. In addition, it is well known that sulfated solid acids ($\text{SO}_4^{2-}/\text{MO}_x$) are potential candidates for the development of environmentally benign organic syntheses. Unfortunately, the activity of these materials decreases significantly during use because of sulfur reduction and the formation of surface

coke [12–15], hindering their industrial applications. Therefore, there is still a need to develop environmentally benign catalysts with high activity.

Typically, these heterogeneous catalysts are separated by labor-intensive filtration or centrifugation processes. Hence, much research has been devoted to the development of easily separable heterogeneous catalysts. Magnetic nanoparticles (MNPs) have been extensively researched with regard to their applications in disciplines, including magnetic resonance imaging [16], magnetic storage media [17], biotechnology [18], and ferrofluids [19]. Among these magnetic materials, Fe_3O_4 nanoparticles have been used as a versatile support for a variety of heterogeneous catalysts in different types of organic transformations [20].

Based on the above factors and our own previous research results [15], we have designed and synthesized several series of “green” solid acids, $\text{TiO}_2\text{-Al}_2\text{O}_3\text{-Fe}_3\text{O}_4$ (TAF), $\text{CeO}_2\text{-Al}_2\text{O}_3\text{-Fe}_3\text{O}_4$ (CAF), and $\text{ZrO}_2\text{-Al}_2\text{O}_3\text{-CeO}_2\text{-Fe}_3\text{O}_4$ (ZACF), each of which

*Corresponding author. Tel/Fax: +86-931-8912585; E-mail: hwjing@lzu.edu.cn

has been applied to the esterification reaction between a carboxylic acid and an alcohol. We subsequently identified the best catalyst (i.e., that exhibiting the highest activity) by varying the molar ratio of different oxides in the catalyst. Furthermore, we propose a plausible mechanism for the esterification reaction based on characterization of the structures and morphologies of these materials.

2. Experimental

2.1. Preparation of catalysts

ZrOCl₂·8H₂O, AlCl₃·6H₂O, Ce(SO₄)₂·4H₂O, *n*-butanol, acetic acid, tetrabutyl titanate, and toluene were all obtained from commercial sources and used as-received without further purification.

Fe₃O₄ MNPs were generated by dissolving FeCl₃·6H₂O (6.76 g) and FeSO₄·7H₂O (3.80 g) in 100 mL of deionized water to produce a clear solution, following which the pH was adjusted to 10 with NH₄OH acting as a precipitant. After 2 h of vigorous stirring at 60 °C, the precipitate was separated magnetically and then washed with deionized water and ethanol. The resulting black, magnetic solid was dried under vacuum at room temperature (Fig. 1).

TAF-4/4 (4/4 means that the molar ratio of TiO₂/Al₂O₃/Fe₃O₄ is 4:4:1) was obtained by dissolving AlCl₃·6H₂O (4 mmol) and tetrabutyl titanate (4 mmol) in 100 mL of ethanol to produce a clear solution, after which Fe₃O₄ MNPs (0.2314 g) were added with ultrasonic agitation for 30 min. NH₄OH was subsequently added as precipitant while adjusting the pH to 9.2. After 12 h of vigorous stirring at room temperature, the precipitate was filtered, washed with deionized water, and dried overnight at 80 °C in a vacuum oven. The remaining nano-magnetic catalysts were also synthesized using this same method.

2.2. Characterization of catalysts

Inductively coupled plasma-atomic emission spectroscopy (ICP-AES) data were collected using an IRIS ER/S emission spectrometer (American TAJ Co.). N₂ adsorption-desorption isotherms were recorded at -195.8 °C on a TriStar II 3020V instrument. The specific surface areas of the materials were calculated using the Brunauer-Emmett-Teller (BET) equation over a range of relative pressure ratios (p/p_0) from 0.06 to 0.3. Powder X-ray diffraction (XRD) patterns were obtained with an X'Pert PRO diffractometer (Holland PANalytical Co.) over the range of $2\theta = 20^\circ$ – 90° at a scan rate of 8°/min using Cu K α radiation ($\lambda = 0.15406$ nm). Transmission electron microscope

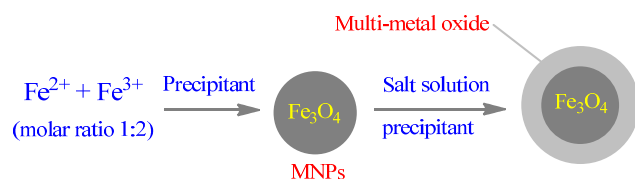
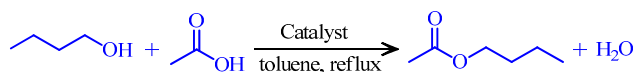


Fig. 1. Preparation of nano-magnetic catalysts.



Scheme 1. Esterification of acetic acid with *n*-butanol.

(TEM) and high resolution TEM (HRTEM) images were obtained using a field emission TEM (Tecnai-G2-F30). Fourier transform infrared (FT-IR) spectra were acquired on a Nicolet NEXUS 670 over the range of 400 to 4000 cm⁻¹ with a resolution of 4 cm⁻¹. Thermal gravimetric (TG) analyses were performed under N₂ from room temperature to 600 °C at a heating rate of 10 °C/min using a Linseis STA PT 1600 thermoanalyzer.

2.3. Typical procedure for the esterification reaction of acetic acid with *n*-butanol

Acetic acid (0.075 mol), *n*-butanol (0.050 mol), catalyst (0.5 g), and 25 mL toluene were combined in a 50 mL flask along with a magnetic bar and water separator. The flask was then immersed in an oil bath and heated to reflux. During the reaction, produced water was separated by the water separator. After the reaction, the catalyst was detached from the flask with magnets for recycling, and the conversion (yield) was determined by GC with FID (Scheme 1)

3. Results and discussion

3.1. Characterization results

The ICP-AES and BET specific surface areas results are shown in Table 1. When preparing TAF, the pH of the solution was approximately 9.2. At this pH, the reaction mixture contained a significant quantity of Al(OH)₄⁻ and Ti(OH)_{*n*}⁻ ions because these species do not precipitate completely at that pH value. The ICP-AES results show some variations between the actual and theoretical molar ratios due to the loss of Al and Ti through the formation of their same ions, as well as the incomplete precipitation of other metal ions at this pH value [21–23].

The XRD patterns of these catalysts are depicted in Fig. 2. In Fig. 2(a), there are only a few weak peaks from Fe₃O₄, showing

Table 1
ICP-AES data and specific surface areas of the catalysts.

Catalyst	ZrO ₂ (TiO ₂)-Al ₂ O ₃ -CeO ₂ -Fe ₃ O ₄ molar ratio		S _{BET} (m ² /g)
	Theoretical	Measured ^a	
TAF-4/4	4:4:0:1	0.98:0.70:0:1	358.72
TAF-8/8	8:8:0:1	1.69:1.28:0:1	256.50
TAF-12/12	12:12:0:1	2.26:1.79:0:1	54.84
TAF-16/16	16:16:0:1	3.26:2.67:0:1	365.99
CAF-8/8	0:8:8:1	0:2.48:0.99:1	196.24
CAF-12/12	0:12:12:1	0:3.84:0.73:1	192.72
CAF-16/16	0:16:16:1	0:5.05:1.42:1	104.56
ZAF-16/16	16:16:0:1	3.99:3.93:0:1	299.26
ZACF-16/16/2	16:16:2:1	4.33:5.36:0.69:1	268.30
ZACF-16/16/4	16:16:4:1	4.41:2.75:1.48:1	288.60
ZACF-16/16/6	16:16:6:1	5.01:4.29:2.05:1	224.05
ZACF-16/14/2	16:14:2:1	4.08:3.43:0.70:1	271.85

^aDetermined by ICP-AES analysis.

Download English Version:

<https://daneshyari.com/en/article/59271>

Download Persian Version:

<https://daneshyari.com/article/59271>

[Daneshyari.com](https://daneshyari.com)